Title	Some Considerations on the Performance of the Esaki-diode Oscillator
Author(s)	Ogawa, Yoshihiko
Citation	Memoirs of the Faculty of Engineering, Hokkaido University, 11(5), 527-557
Issue Date	1964-03
Doc URL	http://hdl.handle.net/2115/37842
Type	bulletin (article)
File Information	11(5)_527-558.pdf

Instructions for use

Some Considerations on the Performance of the Esaki-diode Oscillator

Yoshihiko OGAWA

Contents

Summary

In this paper the hysteresis phenomena and rising time of the oscillation of the Esaki-diode oscillator were analyzed. Also these results were compared with experimental results, from which it can be seen that both results coincide very well.

I. Introduction

It has been frequently observed that considerable hysteresis phenomena are observed in the operation of the Esaki-diode oscillator. In this paper these phenomena are explained to be the results of the shift of the bias voltage, i. e. the origination of the auto-bias voltage, in the state of the oscillation. This explanation coincides well with the experimental results.[2]

Next, in this paper the rising time of the oscillation of the Esaki-diode oscillator was considered. From this consideration it can be seen that the rising time is very short, which shows that the Esaki-diode oscillator is suitable for pulsed oscillation.

II. The Circuit Equations

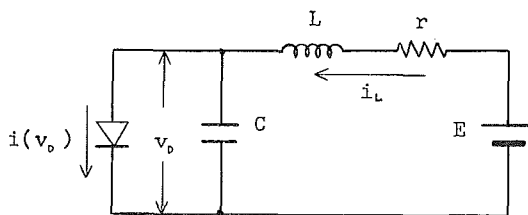The circuit equations corresponding to the circuit of Fig. 1 are

Fig. 1. The circuit of Esaki-diode oscillator.

$$i_{\mathrm{L}} - i(v_{\mathrm{D}}) = C\frac{dv_{\mathrm{D}}}{dt} \tag{1a}$$

and

$$v_{\mathrm{D}} + L\frac{di_{\mathrm{L}}}{dt} + ri_{\mathrm{L}} = E. \tag{1b}$$

Combining the equations (1a) and (1b), we get

$$\frac{d^2 v_{\mathrm{D}}}{d\tau^2} + \frac{1}{Q}\left\{1 + QZ\frac{di(v_{\mathrm{D}})}{dv_{\mathrm{D}}}\right\} + v_{\mathrm{D}} + ri(v_{\mathrm{D}}) = E \tag{2}$$

where

$$\tau = \omega_0 t$$

$$\omega_0 = 1/\sqrt{LC}$$

$$Z = \omega_0 L = \sqrt{L/C}$$

$$Q = (\omega_0 Cr)^{-1} = r^{-1}\sqrt{L/C}$$

Now let

$$v_{\mathrm{D}} \equiv v_{\mathrm{D}0} + v_d \tag{3a}$$

and

$$i(v_{\mathrm{D}}) \equiv i(v_{\mathrm{D}0} + v_d), \tag{3b}$$

where v_{D0} is the bias voltage supplied to the Esaki-diode when L and C were excluded from the circuit of Fig. 1, and v_d is the component of voltage produced in the Esaki-diode only when the circuit of Fig. 1 oscillates. It must be noticed that the d–c component is included in v_d. We rewrite v_d as follows ;

$$v_d \equiv v_{d0} + v \tag{4}$$

where v_{d0} is the d–c component of v_d and v is the alternating component of v_d. v_{d0} is called the auto-bias voltage generated in the oscillatory state.

In the non-oscillatory state, v_a is zero, and Eq. (2) can be written as

$$v_{D0} + ri(v_{D0}) = E .\qquad(5)$$

In the oscillatory state, we shall divide the current flowing in the Esaki-diode into d–c and alternating components as follows;

$$i(v_{D0} + v_a) \equiv i(v_0 + v) \equiv i_a(v_0 + v) + i_d(v_0 + v)\qquad(6)$$

where

$$\left.\begin{array}{l} v_0 \equiv v_{D0} + v_{a0} \\ i_a(v_0 + v): \text{ alternating component} \\ i_d(v_0 + v): \text{ d–c component} \end{array}\right\}.\qquad(7)$$

By using Eq. (6) we can draw the d–c relation of Eq. (2) in the case of steady state as

$$v_0 + ri_d(v_0 + v) = E .\qquad(8)$$

The rest of the relation of Eq. (2) can be rewritten as follows;

$$\frac{d^2 v}{d\tau^2} + v = \varepsilon f\left(v, \frac{dv}{d\tau} ; v_0\right)\qquad(9)$$

where

$$\left.\begin{array}{l} \varepsilon = 1/Q \\[4pt] f\left(v, \dfrac{dv}{d\tau} ; v_0\right) = -\left\{Qri_a(v_0 + v) + \varphi(v ; v_0)\dfrac{dv}{d\tau}\right\} \\[8pt] \varphi(v ; v_0) = 1 + QZ\dfrac{di(v_D)}{dv_D} \end{array}\right\}.\qquad(10)$$

Now we assume that the current $i(v)$ of the Esaki-diode can be approximated as

$$i(v) = \sum_{K=0}^{5} h_K v^K .\qquad(11)$$

By considering Eqs. (5), (8), (9) and (11) we can investigate the oscillatory characteristics of the circuit of Fig. 1.

III. The First Approximation[1]

Assuming that the alternating voltage v may be expressed as

$$v = a\cos\phi\qquad(12)$$

where a and ϕ are the functions of τ and by substituting Eq. (12) into Eq. (8),

we get (see Appendix I)

$$v_0 + r \sum_{K=0}^{5} \sum_{m=0}^{K} h_K \binom{K}{m} \binom{m}{m/2} 2^{-m} \delta_m v_0^{K-m} a^m = E .$$ (13)

Especially in the case of $a=0$, i.e. the non-oscillatory state, we get from the above equation

$$v_{D0} + r \sum_{K=0}^{5} h_K v_{D0}^{K} = E .$$ (14)

This equation is identical with Eq. (5).

Now if we assume that the relationship between a and v_0 can be determined, then from Eq. (13) the source voltage E can be obtained in relation to the values of a and v_0. On the other hand, the relationship between E and v_{D0} can be determined from Eq. (14). From these two results we can compare v_0 with v_{D0} with regards to the same value of E. The difference $v_0 - v_{D0}$ is the auto-bias voltage in the oscillatory state.

Now from Eqs. (10) and (12) the values of a and ψ can be determined, within the limitation of the first approximation, by the next equations (see Appendix II);

$$\frac{da}{d\tau} = \epsilon A_1(a)$$ (15 a)

and

$$\frac{d\psi}{d\tau} = 1 + \epsilon B_1(a)$$ (15 b)

where

$$A_1(a) = -\left\{ F_1(v_0) a + F_3(v_0) a^3 + F_5 a^5 \right\}$$ (16 a)

$$B_1(a) = -\frac{r}{Z} \left\{ \frac{1}{2} + \frac{A_1(a)}{a} \right\}$$ (16 b)

$$F_1(v_0) = \frac{1}{2} \left(1 + QZ \sum_{K=1}^{5} K h_K v_0^{K-1} \right) = \frac{1}{2} \left\{ 1 + QZ g(v_0) \right\}$$ (16 c)

$$F_3(v_0) = \frac{3}{8} QZ \sum_{K=3}^{5} \binom{K}{3} h_K v_0^{K-3}$$ (16 d)

$$F_5 = \frac{5}{16} QZ h_5 .$$ (16 e)

It must be noticed that the value $g(v_0)$ in the Eq. (16 c) is the conductance $di(v_0)/dv_0$ at the point of the operating voltage v_0 of the Esaki-diode.
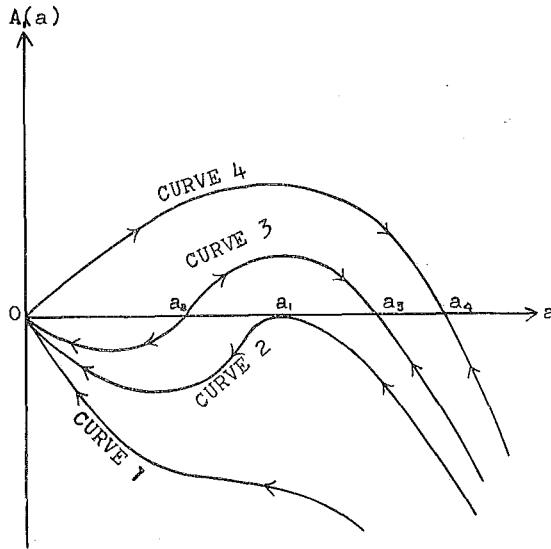
Fig. 2. Four typical curves which may be drawn from
the equation $A_1(a)=0$.

Now considering Eq. (15), it can be seen that the amplitude a is respectively in a damping, growing or steady state corresponding to the negative, positive or zero value of $A_1(a)$. Moreover there are three steady states which are stable, half-stable and unstable. The function $A_1(a)$ can not take the plus value in the region of a sufficiently large value of a from the nature of the Esaki-diode, so that F_5 or h_5 must be positive. Noticing this fact, we can classify the function $A_1(a)$ into four groups which are shown typically with four curves in Fig. 2. The points at which the function $A_1(a)$ crosses with the axis a can be evaluated from the roots of $A_1(a)=0$. These roots are

$$a = 0 \tag{17a}$$

and

$$a = \frac{-F_3 \pm \sqrt{F_3^2 - 4F_1F_5}}{2F_5}. \tag{17b}$$

The nature of stability in steady state can be investigated by determining the sign of the function

$$\frac{dA_1(a)}{da} = -\left\{ F_1(v_0) + 3F_3(v_0)a^2 + 5F_5a^4 \right\} \tag{18}$$

for the real values of a in Eqs. (17). The steady state is stable, half-stable or unstable according to the minus, zero or plus value of Eq. (18) respectively.

Now the origination of oscillation indicates the existence of, at least within the limitation of the first approximation, some limit cycles in the phase plane of $i(v_D)-v_{D0}$. By noticing this fact and investigating the nature of the curves shown in Fig. 2, we can classify the configuration of the trajectories in the phase plane into four types as shown below:

I) There is no limit cycle but only one stable focal point at $a=0$, in the phase plane. In this case the oscillation can not occur. This case corresponds to curve 1 of $A_1(a)-a$ plane, in Fig. 2.

II) There are one stable focal point and one half-stable or outwardly stable limit cycle. This case corresponds to curve 2, in Fig. 2.

III) There are one stable focal point and two limit cycles. One of these two limit cycles is unstable and the other is stable and larger than the unstable limit cycle. This case corresponds to curve 3, in Fig. 2.

IV) There are one unstable focal point and one stable limit cycle. This case corresponds to curve 4, in Fig. 2.

In the first class, there is no real value of a satisfying Eq. (17b) so that either of the next two conditions must be satisfied:

$$F_1(v_{01}) > \frac{F_3^2(v_{01})}{4F_5} \tag{19 a}$$

or

$$F_3(v_{01}) \geqq 0 , \qquad F_1(v_{01}) \geqq 0 . \tag{19 b}$$

Now the condition that the focal point is stable can be decided from Eq. (18) by $[dA_1(a)/da]_{a=0}$, which is

$$F_1(v_{01}) \geqq 0 \tag{20 a}$$

or by rewriting

$$-g(v_{01}) \leqq \frac{1}{QZ} . \tag{20 b}$$

Eq. (20b) shows that the focal point is stable only when the magnitude of the negative conductance of the Esaki-diode at the operating point is not larger than the resonant conductance of the passive circuit excluding the Esaki-diode. It must be noticed that both conditions of Eqs. (19) are satisfied by the condition of Eq. (20b).

In the second class, there is only one positive dual-root a_1 satisfying Eq. (17b), so that the condition

$$F_1(v_{02}) = \frac{F_3^2(v_{02})}{4F_5} , \qquad F_3(v_{02}) < 0 \tag{21}$$

must be satisfied. The dual-root a_1 of this case is

$$a_1 = \frac{-F_3(v_{02})}{2F_5} .$$

(22)

It must be noticed that the condition (21) also satisfies the condition (20 b).

In the third class, there are two positive roots satisfying Eq. (17 b) which are

$$a_2 = \sqrt{\frac{-F_3(v_{03}) - \sqrt{F_3^2(v_{03}) - 4F_1(v_{03})F_5}}{2F_5}}$$

(23 a)

and

$$a_3 = \sqrt{\frac{-F_3(v_{03}) + \sqrt{F_3^2(v_{03}) - 4F_1(v_{03})F_5}}{2F_5}} ,$$

(23 b)

where $a_2 < a_3$.

Now a_2 and a_3 must satisfy two inequalities

$$\left[\frac{dA_1(a)}{da}\right]_{a_2} = -\left\{F_1(v_{03}) + 3F_3(v_{03})a_2^2 + 5F_5a_2^4\right\} > 0$$

(24 a)

and

$$\left[\frac{dA_1(a)}{da}\right]_{a_3} = -\left\{F_1(v_{03}) + 3F_3(v_{03})a_3^2 + 5F_5a_3^4\right\} < 0 .$$

(24 b)

From Eqs. (23 a, b) and (24 a, b) the inequality

$$F_3(v_{03})\sqrt{F_3^2(v_{03}) - 4F_1(v_{03})F_5} < 0$$

(25)

can be deduced. Now it is seen that the inequality (24 a) satisfies the inequality (20 b). By noticing this and the inequality (25) it can be concluded that the condition

$$\frac{F_3^2(v_{03})}{4F_5} > F_1(v_{03}) > 0 > F_3(v_{03})$$

(26)

must be satisfied in this case. Only one stable limit cycle is the one corresponding to a_3.

In the last class, the focal point corresponding to $a = 0$ is unstable so that the next inequality must be satisfied:

$$\left[\frac{dA_1(a)}{da}\right]_{a=0} = -F_1(v_{04}) > 0 .$$

(27)

Next there is one positive single-root satisfying Eq. (17 b) which is

$$a_4 = \sqrt{\frac{-F_3(v_{04}) + \sqrt{F_3^2(v_{04}) - 4F_1(v_{04})F_5}}{2F_5}} \ . \qquad (28)$$

The root a_4 must satisfy the inequality

$$\left[\frac{dA_1(a)}{da}\right]_{a_4} = -\left\{F_1(v_{04}) + 3F_3(v_{04})a_4^2 + 5F_5 a_4^4\right\} < 0 \ . \qquad (29)$$

The inequality (27) satisfies the inequality (29), so that the single condition is

$$F_1(v_{04}) < 0 \qquad (30\,a)$$

or

$$-g(v_{04}) > \frac{1}{QZ} \ . \qquad (30\,b)$$

It is self-evident that the oscillation occurs in the circuit of Fig. 1 when the condition (30 b) is satisfied. But even when this condition can not be satisfied, it is possible, as seen in class III), that the oscillation originates only when the value of the initial condition of a is larger than a_3. This phenomena can be illustrated physically as follows: the oscillation originates when the magnitude of the average negative conductance $\overline{g(a\,;\,v_0)}$ of the Esaki-diode through one cycle of oscillation is not smaller than the resonant conductance $1/QZ$ of the circuit even if the magnitude of the negative conductance at the operating point, $g(v_0)$, is smaller than $1/QZ$.
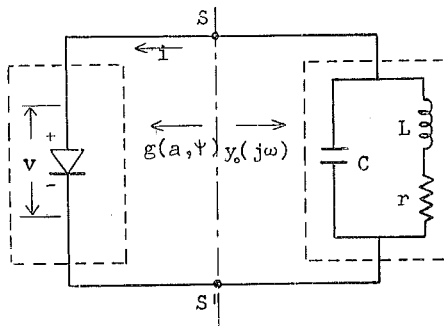
The above conclusion becomes more clear by analyzing the steady-state amplitude and frequency of the circuit shown in Fig. 1 as follows. We will rewrite the circuit shown in Fig. 1 as the one shown in Fig. 3

Fig. 3. Equivalent circuit of Esaki-diode oscillator shown in Fig. 1.

by considering only the r–f component. The admittance $y_0(j\omega)$ in Fig. 3 is

$$y_0(j\omega) = g_0(\omega) + jb_0(\omega)$$
$$= \frac{r}{r^2 + (\omega L)^2} + j\omega\left\{C - \frac{L}{r^2 + (\omega L)^2}\right\} \ . \qquad (31)$$

The admittance of the Esaki-diode $g(a, \phi\,;\,v_0)$ is conductive so far as the first approximation is permitted. The relation between the r–f current i and the r–f voltage v can be shown by using $g(a, \phi\,;\,v_0)$ as

$$i = g(a, \phi; v_0) \cdot v . \tag{32}$$

It must be noticed that the conductance $g(a, \phi; v_0)$ is the function of the phase ϕ or normalized time τ. Now if we assume that the oscillation can occur only when the next relation is satisfied between the conductance $y_0(j\omega)$ and the average conductance $\overline{g(a; v_0)}$ of $g(a, \phi; v_0)$ through one cycle of oscillation;

$$\overline{g(a; v_0)} + y_0(j\omega) = 0 , \tag{33}$$

or by rewriting

$$\overline{g(a; v_0)} + \frac{r}{r^2 + (\omega L)^2} = 0 \tag{34 a}$$

and

$$C - \frac{L}{r^2 + (\omega L)^2} = 0 . \tag{34 b}$$

From Eq. (34 b) the angular frequency can be obtained as

$$\omega = \frac{1}{\sqrt{LC}} \cdot \sqrt{1 - \frac{Cr^2}{L}} . \tag{35}$$

The above value coincides with the one obtained from Eq. (15 b) within the limitation of the first approximation.

Next using by Eq. (35), Eq. (34 a) can be rewritten as follows;

$$\overline{g(a; v_0)} + \frac{1}{QZ} = 0 . \tag{36}$$

This is the relation deciding the r–f amplitude.

Now $\overline{g(a; v_0)}$ can be calculated as follows;

$$
\begin{aligned}
\overline{g(a; v_0)} &= \frac{1}{\pi a} \int_0^{2\pi} i(a \cos \phi; v_0) \cos \phi \, d\phi \\
&= \frac{1}{\pi a} \int_0^{2\pi} \sum_{K=0}^{5} h_K (v_0 + a \cos \phi)^K \cos \phi \, d\phi \\
&= \sum_{K=1}^{5} K h_K v_0^{K-1} + \left(h_3 + 4 h_4 v_0 + 10 h_5 v_0^2 \right) \cdot \frac{3}{4} a^2 + \frac{5}{8} h_5 a^4 \\
&= g(v_0) + \frac{2}{QZ} \left\{ F_3(v_0) a^2 + F_5 a^4 \right\} .
\end{aligned} \tag{37 a}
$$

Eliminating $\overline{g(a; v_0)}$ from Eq. (36) and Eq. (37 a), we can obtain the same condition obtained from $A_1(a) = 0$ (see Eq. (16 a)).

It is interesting to rewrite Eq. (37 a) as

$$-\{\overline{g(a;\ v_0)}-g(v_0)\} = -\frac{2}{QZ}\{F_3(v_0)a^2+F_5a^4\}\ . \qquad (37\,\mathrm{b})$$

If

$$a^2 < -\frac{F_3(v_0)}{F_5}\ , \qquad\qquad (38)$$

then the right hand side of Eq. (37 b) is positive, so that the magnitude of the average negative conductance becomes larger than that of the negative conductance in the operating point. Noticing this fact and Eq. (36), we can conclude that the oscillations can originate even when the inequalities

$$-\overline{g(a;\ v_0)} > \frac{1}{QZ} > -g(v_0) \qquad\qquad (39)$$

are satisfied at the r-f amplitude a satisfying the inequality (38). The above condition coincides with that of the hard oscillation shown in Eq. (26).

Now we will take the numerical examples:

$$\left.\begin{array}{l} h_0 = 0.3216858856 \times 10^{-3} \\ h_1 = 0.7153101565 \times 10^{-1} \\ h_2 = -0.9813351377 \times 10^{0} \\ h_3 = 0.5063747180 \times 10^{1} \\ h_4 = -0.1153375937 \times 10^{2} \\ h_5 = 0.9760796488 \times 10^{1} \end{array}\right\} \qquad\qquad (40\,\mathrm{a})$$

and

$$C = 350\ \mathrm{p.F.}\ , \qquad L = 1\ \mu\mathrm{H}\ , \qquad\qquad (40\,\mathrm{b})$$

where h_i $(i=0\sim5)$ are the coefficients used in Eq. (11), and C and L are the capacitance and the inductance shown in Fig. 1. The static current-voltage characteristics approximated by Eq. (40 a) is compared with the one measured, in Fig. 4.

Now it is convenient to define the next function:

$$\xi(v_0) = \frac{1}{QZ}\left\{2F_1(v_0)-1-\frac{F_3^2(v_0)}{2F_5}\right\}\ . \qquad\qquad (41)$$

By rewriting Eq. (16 c), $g(v_0)$ is

$$g(v_0) = \frac{1}{QZ}\{2F_1(v_0)-1\}\ . \qquad\qquad (16\,\mathrm{c}')$$

For the above numerical example, $\xi(v_0)$ and $g(v_0)$ are shown in Fig. 5. The
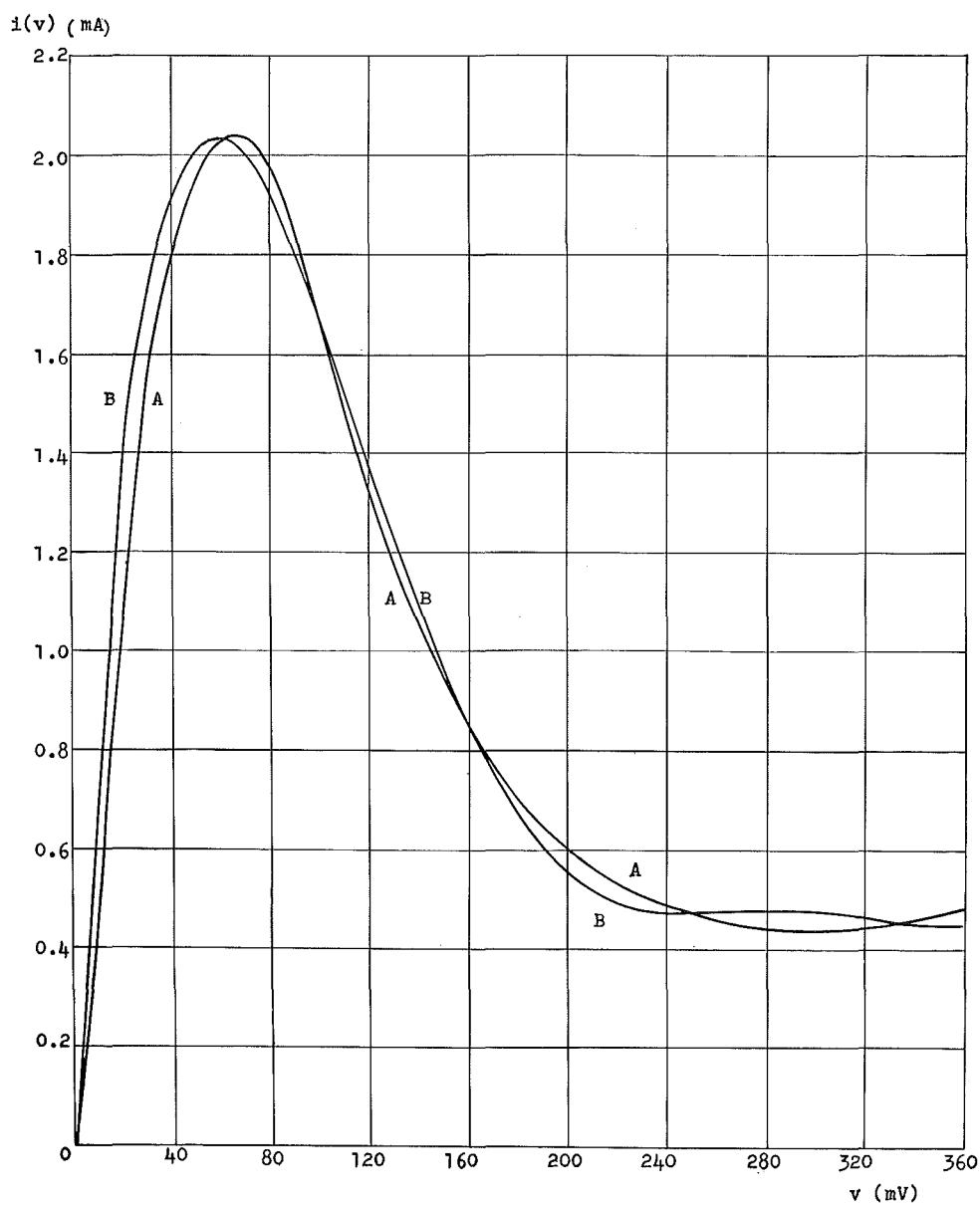
i(v) (mA)

Fig. 4. Comparison between the approximated $v-i$ characteristic (B) and the measured one (A), of Esaki-diode.

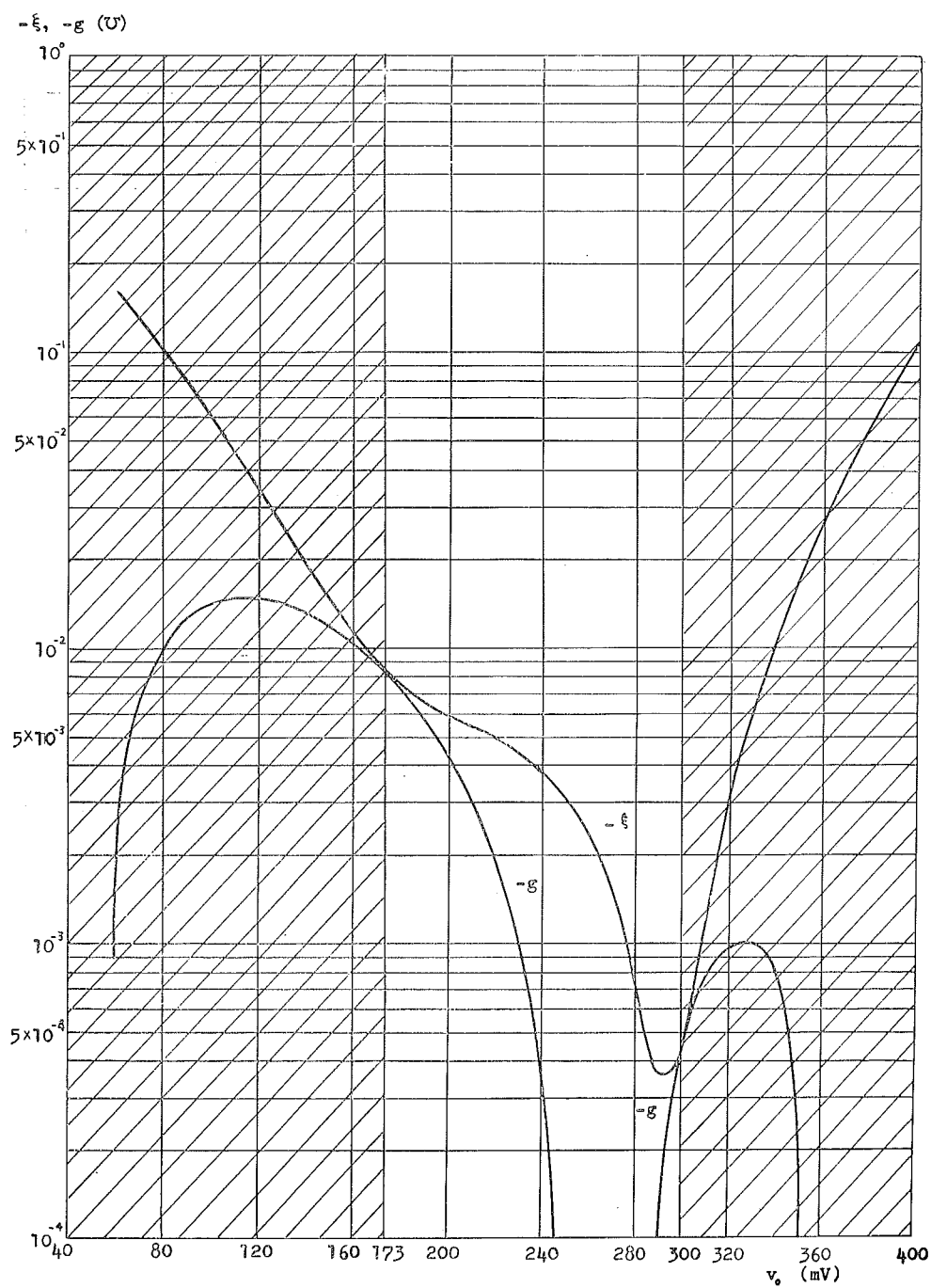**Fig. 5.** $-\xi$ and $-g$ plotted as a function of v_0. Hatched regions show $F_3 > 0$.

regions satisfying the inequality

$$F_3(v_0) < 0 \,,\tag{42 a}$$

or

$$\frac{-2h_4 - \sqrt{4h_4^2 - 10h_3h_5}}{h_3} < v_0 < \frac{-2h_4 + \sqrt{4h_4^2 - 10h_3h_5}}{h_3} \,,\tag{42 b}$$

is shown at the same time in Fig. 5.

By using $\xi(v_0)$, $g(v_0)$ and $F_3(v_0)$, the conditions (19 a), (19 b), (21), (26) and (30 a) are respectively rewritten as follows;

$$-\xi(v_0) < \frac{1}{QZ} \,,\tag{19 a'}$$

$$-g(v_0) \leqq \frac{1}{QZ} \,, \qquad F_3(v_0) \geqq 0 \,,\tag{19 b'}$$

$$-\xi(v_0) = \frac{1}{QZ} \,, \qquad F_3(v_0) < 0 \,,\tag{21'}$$
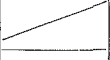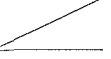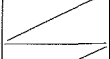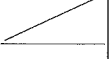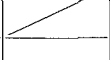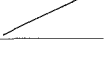
$$-\xi(v_0) > \frac{1}{QZ} > -g(v_0) \,, \qquad 0 > F_3(v_0)\tag{26'}$$

and

$$-g(v_0) \geqq \frac{1}{QZ} \,.\tag{30 a'}$$

In Table 1 the above conditions are all collected and compared with the number of curve in Fig. 2. We will show one example of using Fig. 5 and Table 1 in the case of $1/QZ = 2 \times 10^{-3}\,\mho$. First draw the straight line parallel to the horizontal axis corresponding to $2 \times 10^{-3}\,\mho$. Next compare this line with values of $-\xi(v_0)$ and $-g(v_0)$. By refering Table 1, the conclusion

TABLE 1.

Classified number	I	II	III	IV	V
$-\xi - 1/(QZ)$	$-$		0	$+$	
$-g - 1/(QZ)$		$-,\ 0$		$-$	$+,\ 0$
F_3		$+,\ 0$	$-$	$-$	
Curve number in Fig. 2 corresponding to the above condition.	1	1	2	3	4

shown in Table 2 can be dedcued.

<div align="center">TABLE 2.</div>

v_0 (mV)	classified No.	state of oscillation
$v_0 \leqq 71$	II	no osc.
$71 < v_0 \leqq 219$	V	free osc.
$219 < v_0 < 264$	IV	hard osc.
264	III	half stable osc.
$264 < v_0 < 315$	I	no osc.
$v_0 \geqq 315$	II	no osc.

It is plausible to think that there is a hysteresis phenomena with regard to the characteristics of the r–f amplitude a versus the operating voltage v_0 of the Esaki-diode as far as the hard oscillation is concerned. In the above example, by increasing v_0 the oscillation disappears for $v_0 = 264$ mV. Next for decreasing v_0 from this value it is observed, however, that the oscillation does not occur for $v_0 > 219$ mV and it occurs at $v_0 = 219$ mV.

It is questionable, however, to believe that the above conclusion is right. Because in the above conclusion, the fact that d–c current-voltage characteristics of the Esaki-diode in the oscillatory state differs from the one in the static state is neglected. This difference is shown in Fig. 6. The static characteristic can be drawn by using Eq. (11) which is

$$i(v_0) = \sum_{K=0}^{5} h_K v_0^K .$$

Those in the oscillatory state can be drawn by considering Eq. (8) and Eq. (13); namely d–c current $i_d(v_0 + v)$ is

$$i_d = \sum_{K=0}^{5} \sum_{m=0}^{K} h_K \binom{K}{m} \binom{m}{m/2} \cdot 2^{-m} \delta_m v_0^{K-m} a^m , \tag{43}$$

where the relation between the r–f amplitude a and the operating voltage v_0 can be obtained from Eq. (17b). From Fig. 6 the following interesting conclusions can be introduced: First, in the state of curve B the oscillation disappears continuously with increasing v_0 at the point Q_1 where the curve B meets with the curve A which shows the static characteristic. This fact means that the hysteresis phenomena can not occur. But in the state of the curve C the oscillation disappears discontinuously at point Q_2 with increasing v_0 and the operating point of the Esaki-diode jumps to point Q_2'. Next, for decreasing v_0 from this value the operating point of the Esaki-diode follows the static
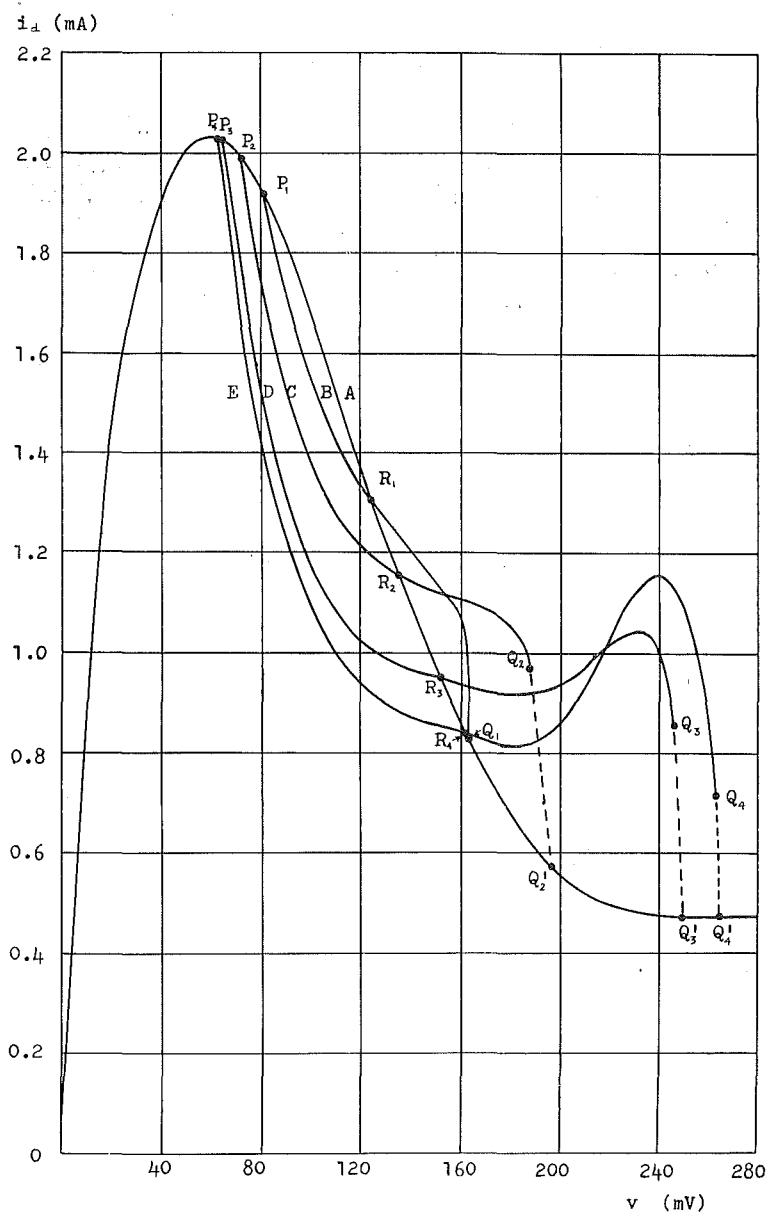
Fig. 6. Some i_d-v characteristics of a Esaki-diode; A: the static characteristic, B~E: the characteristics in the oscillatory state (B: $QZ=100\,\Omega$, $r=27.57\,\Omega$, C: $QZ=150\,\Omega$, $r=19.05\,\Omega$, D: $QZ=300\,\Omega$, $r=9.524\,\Omega$, E: $QZ=500\,\Omega$, $r=5.714\,\Omega$)

characteristic line A to the point R where it shifts on the curve C and the oscillation occurs again. The same hysteresis phenomena appear in the case of the curves D and E.

We must also consider the hysteresis phenomena with regard to the characteristics of the r–f amplitude a versus the source voltage E instead of the operating voltage v_0 of the Esaki-diode as shown above. We will plot the characteristics of v_0 and v_{D0} versus E which can be obtained from Eqs. (13) and (14) respectively. These are shown in Fig. 7, Fig. 8, Fig. 9 and Fig. 10 for some cases of QZ and r. For example, it can be seen from Fig. 8 that
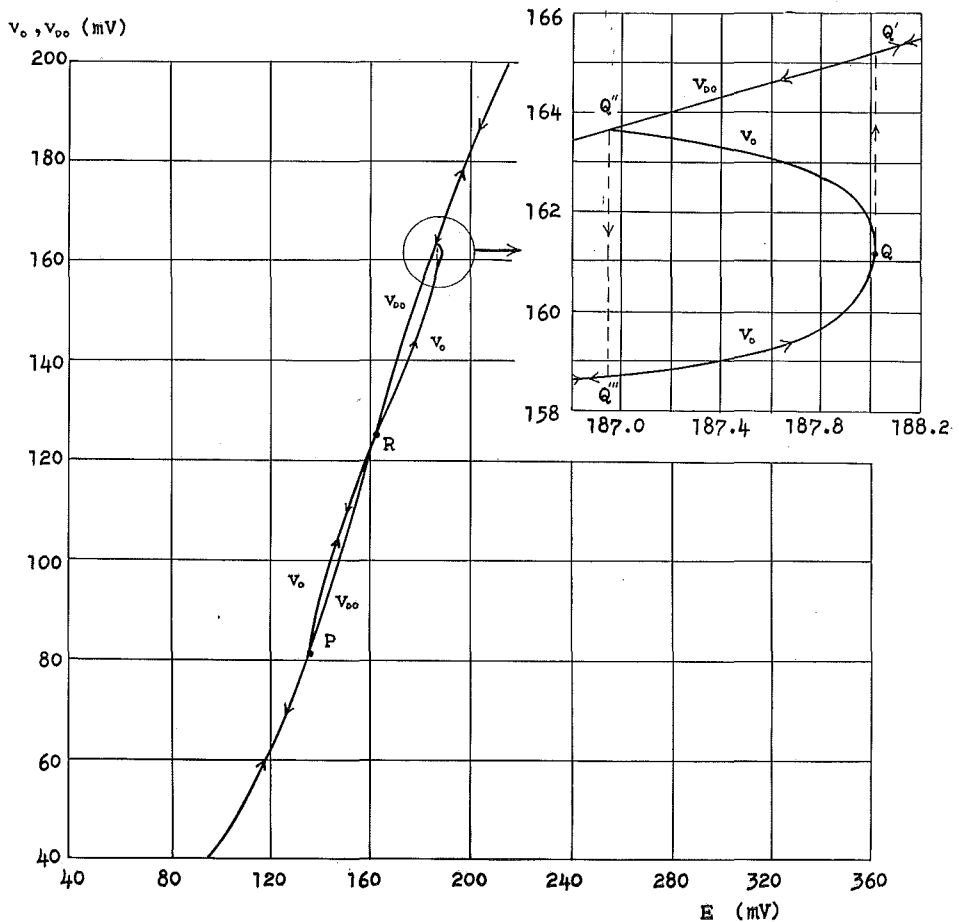

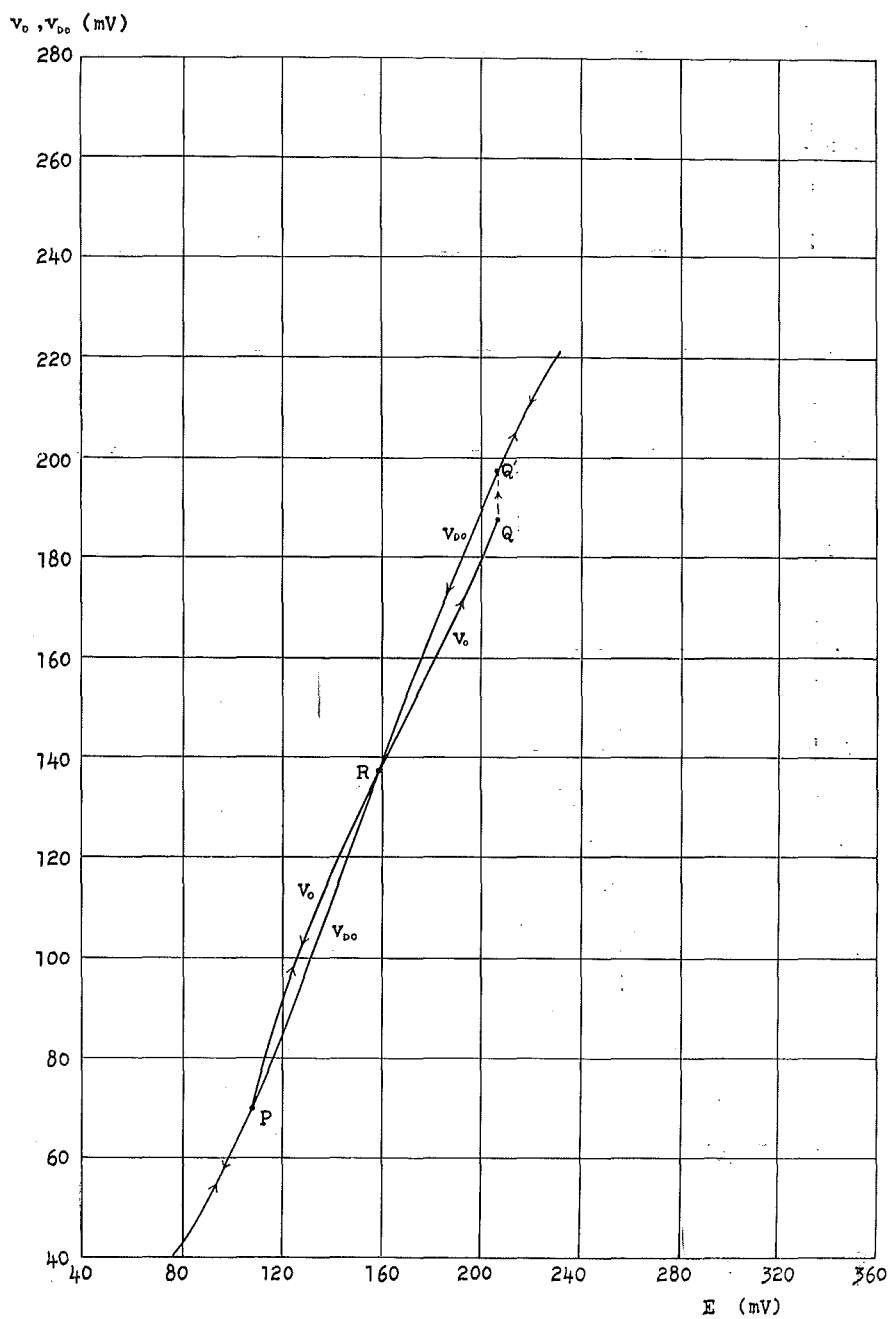Fig. 7. v_0 and v_{D0} plotted as a function of E for the case of $QZ = 100\,\Omega$ and $r = 27.57\,\Omega$.

v_0 , v_{D0} (mV)

Fig. 8. v_0 and v_{D0} plotted as a function of E for the case
of $QZ = 150\,\Omega$ and $r = 19.05\,\Omega$.
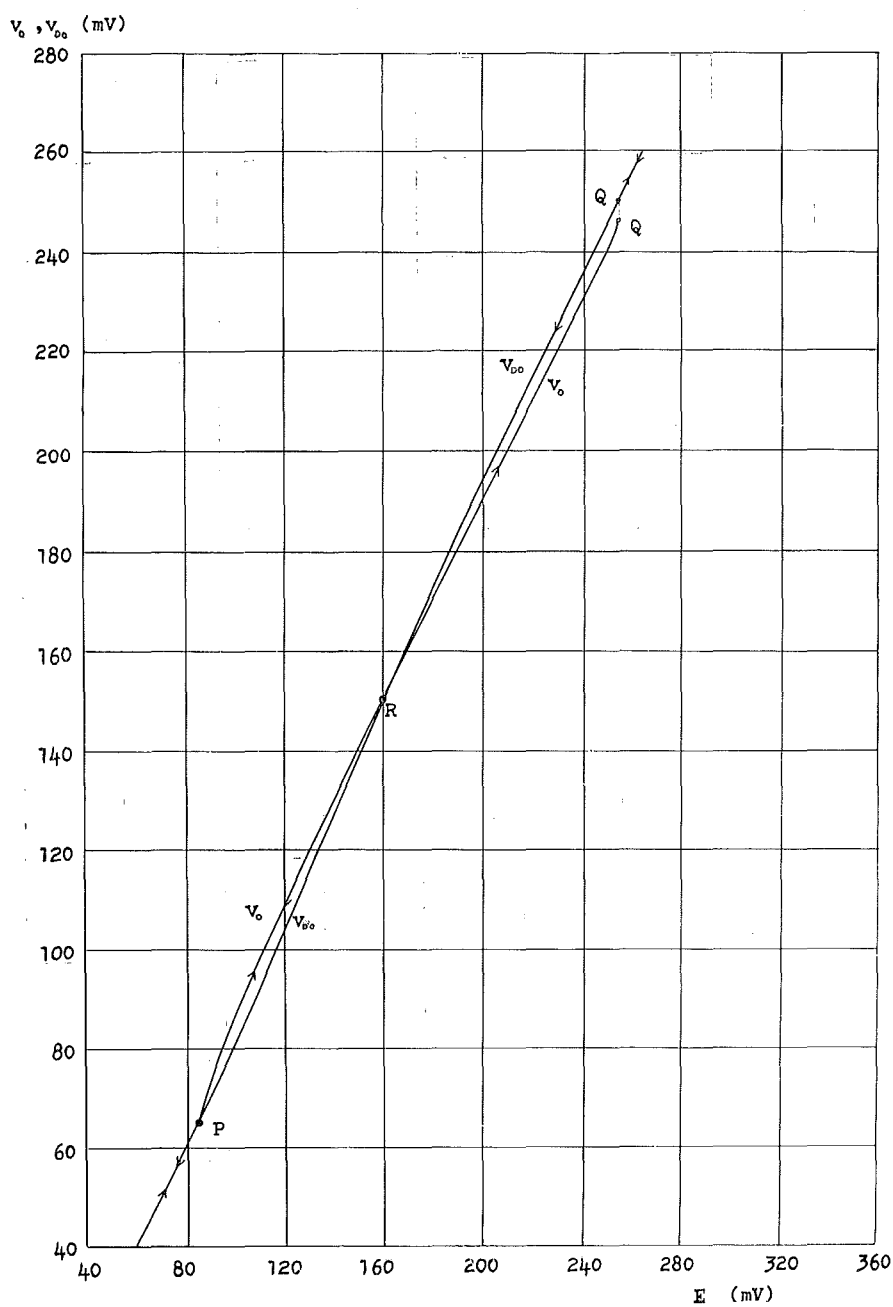
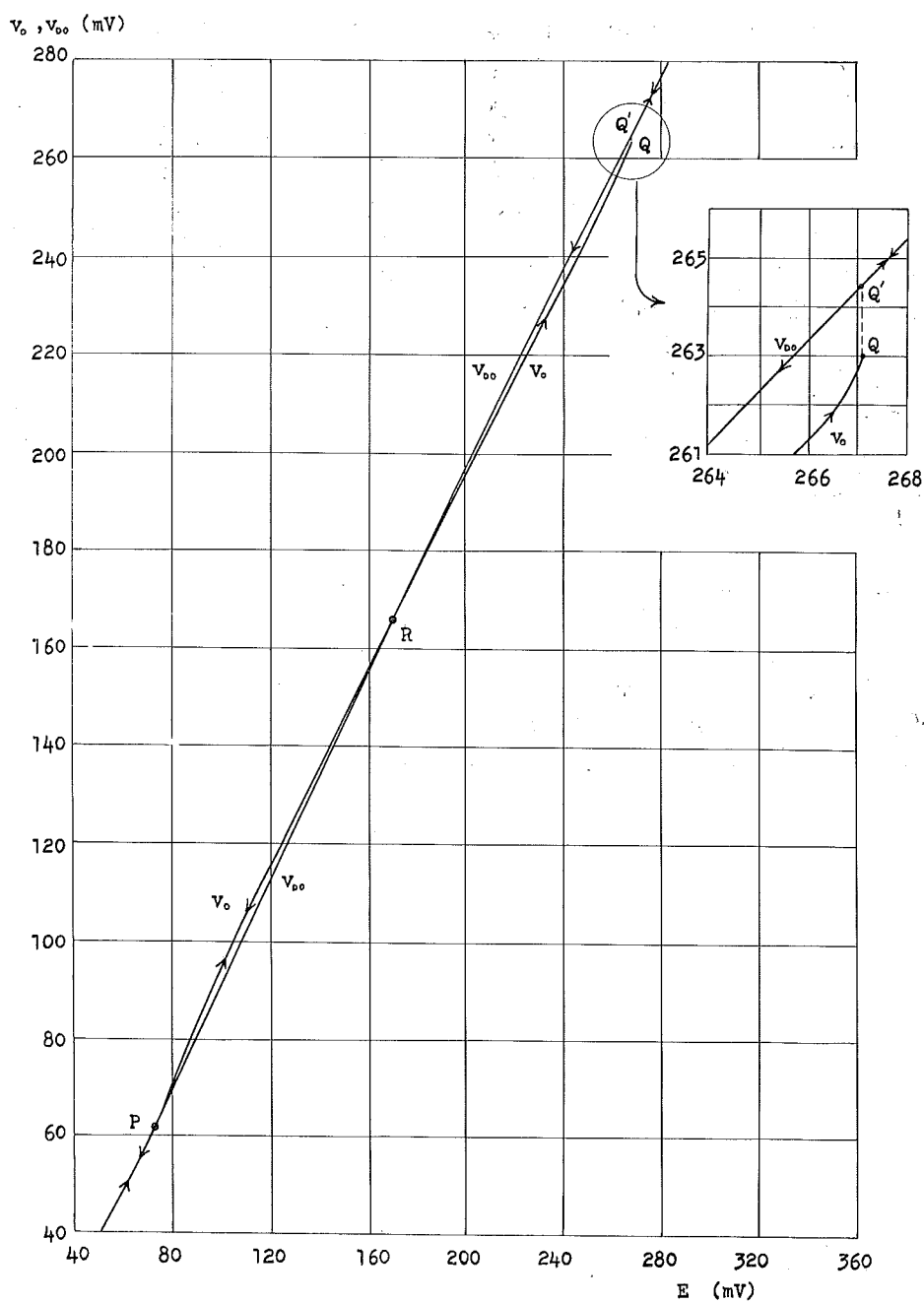**Fig. 9.** v_0 and v_{D0} plotted as a function of E for the case of $QZ = 300\,\Omega$ and $r = 9.524\,\Omega$.

V_o , V_{Do} (mV)

Fig. 10. v_0 and v_{Do} plotted as a function of E for the case
of $QZ = 500\,\Omega$ and $r = 5.714\,\Omega$.

E (mV)

by increasing E the oscillation disappears discontinuously at the point Q where the operating voltage of the Esaki-diode jumps to the point Q', and that for decreasing E from this value, the operating voltage of the Esaki-diode follows the v_{D0}-line and the oscillation can not occur till the point R. The difference $(v_0 - v_{D0})$ is the auto-bias voltage of the Esaki-diode in the oscillatory state. This value is much smaller in the case of Fig. 10 when compared with the case of Fig. 8. In such cases, the operating voltage of the Esaki-diode might accidentally jump from some point on the v_{D0}-line to another point on the v_0-line by the external noise-voltage affecting the Esaki-diode directly. In this case, the oscillation might occur unexpectedly.

It is interesting to note the case of Fig. 7, where there are two values of v_0 corresponding to one value of E in the narrow range of it. In this case, by increasing E the oscillation disappears discontinuously at point Q, and the operating point of the Esaki-diode jumps to the point Q'. Next for decreasing E from this value, the operating point follows the v_{D0}-line, and the oscillation occurs at point Q'' so that the operating point jumps to the point Q'''. ·

Finally we will plot the relations of the r–f amplitude a versus v_0 and the same value versus E in Fig. 11 and Fig. 12 respectively, which have been also utilized in the above analysis. Fig. 13 is the comparison between the experimental and theoretical values of the r–f amplitude a versus E in the case of $QZ = 300 \ \Omega$ and $r = 9.524 \ \Omega$. So far as the r–f amplitude is concerned, both curves coincide approximately in the region of the large value of E though
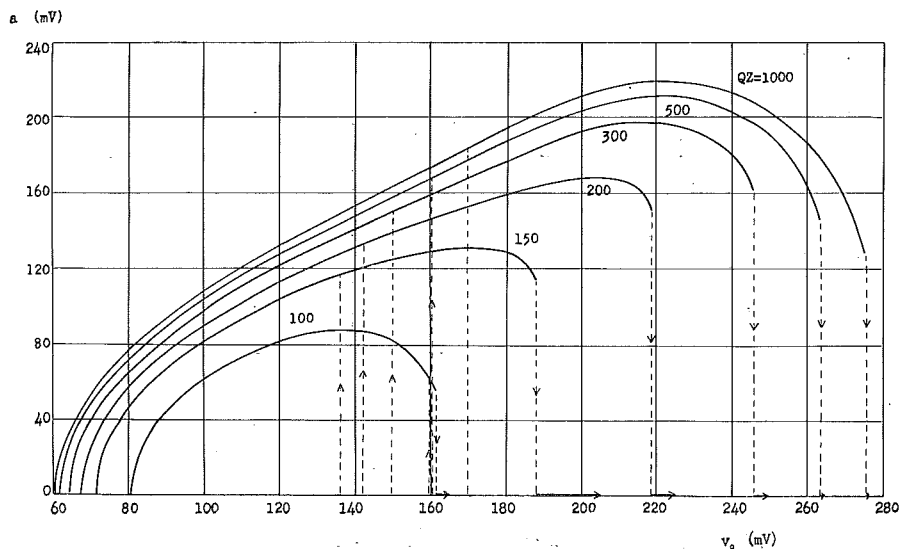

Fig. 11. The r–f amplitude a as a function of v_0 for many cases of QZ.
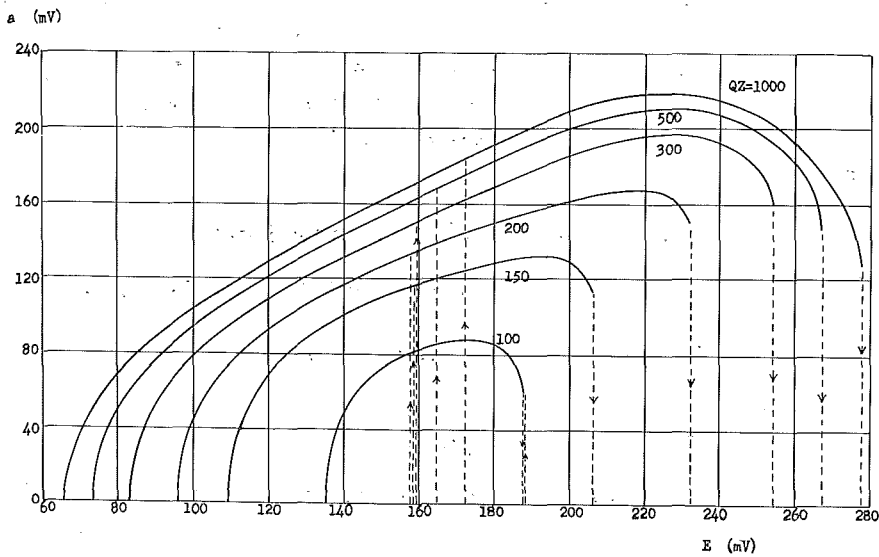
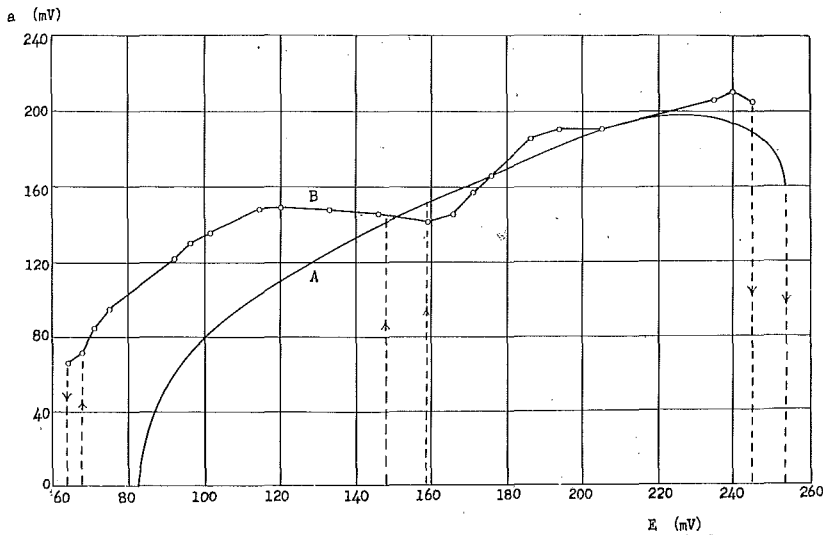**Fig. 12.** The r-f amplitude a as a function of E
for many cases of QZ.

Fig. 13. Comparison between the theoretical (A) and experimental
(B) values of the r-f amplitude a as a function of E with
the same value of QZ and r which are $300\,\Omega$ and $9.524\,\Omega$
respectively.

they do not coincide in the region of the small value of E which may be due to the existence of the higher harmonics. So far as the hysteresis phenomena are concerned, both curves coincide approximately, except for the region of the small value of E where a slight hysteresis phenomena exists in the experimental curve which can not be illustrated in the scope of the first approximation.

IV. The Second Approximation[1)]

It is convenient to utilize the following analysis for obtaining the second-approximated solution.

We put the first-approximated r–f voltage v of the Esaki-diode as

$$v = a \cos \phi$$
$$\phi = \omega t + \varphi .$$

The current flowing into the Esaki-diode by this voltage can be expanded into Fourier series as

$$i = i(a \cos \phi ; \ v_0) = \sum_{n=0}^{5} i_n(a ; \ v_0) \cos n\phi , \tag{44}$$

where $i_n(a ; \ v_0)$ are shown in Appendix III.

Now by the current component $i_n(a ; \ v_0) \cos n\phi$, the voltage

$$y_0(p)^{-1} i_n(a ; \ v_0) \cos n\phi \tag{45}$$

is produced at both ends of $y_0(p)$ $(p \equiv d/dt)$ shown in Fig. 3.

Put

$$y_0(j\Omega) = |y_0(\Omega)| e^{j\phi(\Omega)} = g_0(\Omega) + jb_0(\Omega) , \tag{46}$$

where

$$\left.\begin{aligned}
|y_0(\Omega)| &= \sqrt{g_0^2(\Omega) + b_0^2(\Omega)} \\
g_0(\Omega) &= \frac{r}{r^2 + (\Omega L)^2} \\
b_0(\Omega) &= \Omega \left\{ C - \frac{L}{r^2 + (\Omega L)^2} \right\} \\
\cos \phi &= \frac{g_0(\Omega)}{\sqrt{g_0^2(\Omega) + b_0^2(\Omega)}} \\
\sin \phi &= \frac{b_0(\Omega)}{\sqrt{g_0^2(\Omega) + b_0^2(\Omega)}}
\end{aligned}\right\} , \tag{47}$$

then Eq. (45) can be rewritten as

$$y_0^{-1}(j\Omega)\, i_n(a\,;\,v_0)\cos n\phi$$

$$=\frac{i_n(a\,;\,v_0)}{\sqrt{g_0^2(\Omega)+b_0^2(\Omega)}}\cdot\cos\left\{n\omega t+n\varphi-\phi(n\omega)\right\}; \tag{48}$$

so that the formula of v in the second approximation is

$$v=a\cos\phi+\sum_{n\neq1}\frac{i_n(a\,;\,v_0)}{\sqrt{g_0^2(n\omega)+b_0^2(n\omega)}}\cdot\cos\left\{n\phi-\phi(n\omega)\right\}$$

$$=a\cos\phi+\varDelta, \tag{49}$$

where

$$\varDelta\equiv\sum_{n\neq1}\frac{i_n(a\,;\,v_0)}{\sqrt{g_0^2(n\omega)+b_0^2(n\omega)}}\cdot\cos\left\{n\phi-\phi(n\omega)\right\}.$$

Generally Eq. (49) is utilizable only if

$$\left|\frac{i_n(a\,;\,v_0)}{\sqrt{g_0^2(n\omega)+b_0^2(n\omega)}}\right|\ll a, \qquad n\neq1. \tag{50}$$

The current i can be calculated more precisely by using Eq. (49), and can be expanded into Fourier series as

$$i=i(a\cos\phi+\varDelta)$$

$$\fallingdotseq i(a\cos\phi)+\varDelta\cdot i'(a\cos\phi)$$

$$=\sum_{n=0}^{5}i_n(a)\cos n\phi+I_0(a)$$

$$+\sum_{n=1}^{5}\left\{I_{cn}(a)\cos n\phi+I_{sn}(a)\sin n\phi\right\}, \tag{51}$$

where $I_{cn}(a)$ and $I_{sn}(a)$ are shown in Appendix IV.

Now if we consider that the fundamental component of the right hand side of Eq. (51) is equal to the fundamental component of the current flowing into the linear element $y_0(j\omega)$, then we have

$$-y_0(j\omega)a\cos(\omega t+\varphi)=-|y_0(\omega)|\,a\cos\left\{\omega t+\varphi+\phi(\omega)\right\}$$

$$=i_1(a)\cos(\omega t+\varphi)+I_{c1}(a)\cos(\omega t+\varphi)$$

$$+I_{s1}(a)\sin(\omega t+\varphi),$$

so that

$$-|y_0(\omega)|\,a\cos\phi(\omega)=i_1(a)+I_{c1}(a) \tag{52a}$$

and

$$|y_0(\omega)|\,a\sin\phi(\omega)=I_{s1}(a), \tag{52b}$$

where (see Appendix IV)

$$I_{c1}(a) = \frac{1}{2} \sum_{n \ne 1} \frac{1}{|y_0(n\omega)|} \cdot \frac{d i_n^2(a)}{da} \cdot \cos \phi(n\omega) \qquad (53\,a)$$

and

$$I_{s1}(a) = \sum_{n \ne 0,1} \frac{1}{|y_0(n\omega)|} \cdot \frac{n i_n^2(a)}{a} \cdot \sin \phi(n\omega) . \qquad (53\,b)$$

From Eqs. (52 a, b) and Eqs. (53 a, b) the r–f amplitude a and the angular frequency ω can be calculated in the scope of the second approximation.

V. The Rising Time of the Oscillation

From Eqs. (15 a) and (16 a),

$$\frac{da}{\dfrac{F_1(v_0)}{F_5} a + \dfrac{F_3(v_0)}{F_5} a^3 + a^5} = -\epsilon F_5 d\tau . \qquad (54)$$

Hereafter, we restrict the oscillatory condition to the case where only one stable oscillation exists. This condition is (see Eq. (27))

$$F_1(v_0) < 0 . \qquad (55)$$

Now put

$$a_4^2 = \frac{-F_3(v_0) + \sqrt{F_3^2(v_0) - 4F_1(v_0)F_5}}{2F_5} , \qquad a_4 > 0 \qquad (56\,a)$$

and

$$b_4^2 = \frac{F_3(v_0) + \sqrt{F_3^2(v_0) - 4F_1(v_0)F_5}}{2F_5} , \qquad b_4 > 0 . \qquad (56\,b)$$

Eq. (54) can be rewritten by using Eqs. (56 a, b) as

$$\frac{da}{a(a^2 - a_4^2)(a^2 + b_4^2)} = -\epsilon F_5 d\tau .$$

By integrating this equation,

$$\frac{a}{(a_4^2 - a^2)^{m_1}(b_4^2 + a^2)^{m_2}} = C_0 \exp\left[-\epsilon F_1(v_0)\tau\right] , \qquad (57)$$

where C_0 is the integral constant, and m_1 and m_2 are

$$m_1 = \frac{b_4^2}{2(a_4^2 + b_4^2)}$$

$$m_2 = \frac{a_4^2}{2(a_4^2 + b_4^2)} .$$

Now let the r-f amplitude at $\tau = 0$ be a_0, and this at $\tau = \tau$ be

$$a = \eta(\tau)a_4, \quad 1 \geqq \eta(\tau) > \frac{a_0}{a_4} = \eta_0 . \tag{58}$$

Then

$$C_0 = \frac{a_0}{(a_4^2 - a_0^2)^{m_1}(b_4^2 + a_0^2)^{m_2}} . \tag{59}$$

Eq. (57) can be rewritten by using Eq. (58) and (59) as

$$\frac{\eta}{a_4^{2m_1-1}(1-\eta^2)^{m_1}(b_4^2 + a_4^2\eta^2)^{m_2}} = C_0 \exp[-\epsilon F_1 \tau], \tag{57'}$$

or

$$\tau = \frac{1}{-\epsilon F_1}\left\{\ln\frac{\eta}{\eta_0} - m_1\ln\frac{1-\eta^2}{1-\eta_0^2} - m_2\ln\frac{1-(1-\eta^2)\cdot 2m_2}{1-(1-\eta_0^2)\cdot 2m_2}\right\}. \tag{57''}$$

The first term of the right hand side in Eq. (57'') shows the initial state in the rising of the oscillation. This can also be obtained with the linear-approximated differential equation of the circuit shown in Fig. 1. The second term of the right hand side in Eq. (57'') shows the latter state in the rising of the oscillation. This shows the saturated characteristics in the oscillation. The last term of the right hand side in Eq. (57'') is a corrective term and is of little importance.

Now we define the rising time τ_s of the oscillation as

$$\tau_s = [\tau]_{\eta=0,9} - [\tau]_{\eta=0,1} . \tag{58}$$

Then by using Eq. (57''), τ_s is

$$\tau_s = \frac{-1}{\epsilon F_1}\left(\ln 9 + m_1\ln\frac{99}{19} - m_2\ln\frac{1-0.38m_2}{1-1.98m_2}\right). \tag{59}$$

By rewriting Eq. (59),

$$\tau_s Z = t_s\omega_0 Z = \Gamma(v_0, QZ), \tag{60}$$

where

$$\Gamma(v_0, QZ) = \frac{-2}{\dfrac{1}{QZ} + g(v_0)}\left[2.197 + 1.650m_1 - m_2\ln\frac{1-0.38m_2}{1-1.98m_2}\right]. \tag{61}$$

(Note that m_1 and m_2 are both functions of v_0 and QZ). The next relation has been used in calculation of Eq. (60);
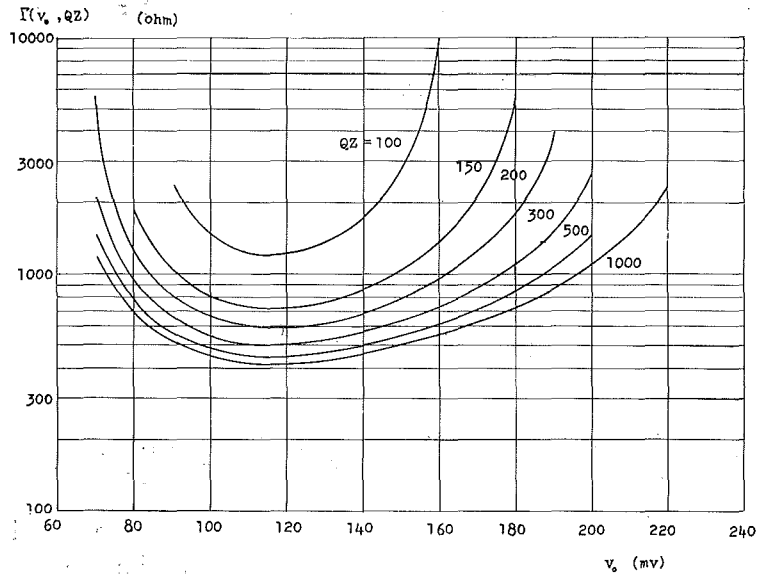
Fig. 14. $\Gamma(v_0, QZ)$ plotted as a function of v_0.

$$\epsilon = 1/Q, \qquad Q = r^{-1}\sqrt{L/C}$$

$$\omega_0 Z = 1/C, \qquad Z = \sqrt{L/C}, \qquad \omega_0 = 1/\sqrt{LC}$$

$$\tau_s = \omega_0 t_s$$

$$F_1(v_0) = \frac{1}{2}\left\{1 + QZg(v_0)\right\}$$

$\Gamma(v_0, QZ)$ are plotted in Fig. 14 as a function of v_0 in some cases of QZ.

If QZ, Z and ω_0 are determined, then three circuit elements L, C and r can be decided. Assume that QZ and ω_0 are decided. Then the larger Z is, the shorter the rising time of the oscillation is. Next assume that Zr and ω_0 are decided. Then the larger the resonant impedance QZ is, the shorter the rising time is. Lastly assume that QZ, Z and ω_0 are all decided. Then the rising time is the shortest in the neighborhood of $v_0 = 120$ mV.

We will take one numerical example:

$$L = 1\,\mu\text{H}, \qquad C = 350\,\text{p.F.}, \qquad r = 5.714\,\Omega$$

$$v_0 = 120\,\text{mV}$$

$$\omega_0 = 5.35 \times 10^7\,\text{rad/sec}\ (f_0 = 8.5\,\text{MC})$$

$$Z = 53.5\,\Omega, \qquad QZ = 500\,\Omega.$$

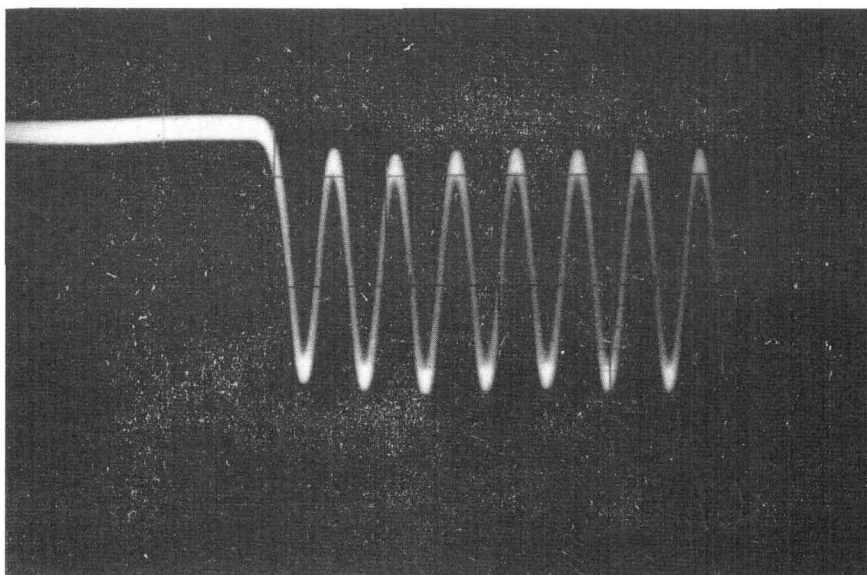In this case, by referencing Fig. 14,

Fig. 15. The initial state of oscillation of the Esaki-diode oscillator :
$\Gamma = 1 \, \mu H$, $C = 350 \, \text{p.F.}$ and $r = 6 \, \Omega$.

$$f_0 t_s = \frac{\Gamma(v_0, \, QZ)}{2\pi Z} = 1.36 \; \text{cycle} . \tag{63}$$

From Eq. (63) it can be seen that the rising time of the Esaki-diode oscillator is fairly short.   The experimental results of the rising time using the same circuit constants shown above is shown in Fig. 15.   This photograph supports the analysis which was conducted previously.

VI. Conclusion

The hysteresis phenomena of the Esaki-diode oscillator are observed experimentaly in two regions of bias voltages, i. e. small bias voltages and large bias voltages.   The latter can be illustrated from the first approximated analysis of the non-linear differential equation, the results of which adequately coincide with the experimental results.   But the former can not be illustrated within the scope of the first approximation.   However it may be illustrated from the second approximation.

It can be seen from both the analysis and the experiments that the rising time of the oscillation of the Esaki-diode oscillator is considerably short.   This result shows that the Esaki-diode oscillator is suitabled for pulsed oscillation.

Acknowledgment

The author wishes to thank Prof. Teiichi Kurobe and his staff of the department of electronic engineering, Hokkaido University, for their valuable suggestions and constructive criticisms.

Appendix I

$$i(v_0 + a \cos \phi) = \sum_{K=0}^{5} h_K (v_0 + a \cos \phi)^K$$

$$\doteqdot \sum_{K=0}^{5} \sum_{m=0}^{K} h_K v_0^{(K-m)} a^m \binom{K}{m} \cos^m \phi$$

$$= \sum_{K=0}^{5} \sum_{m=0}^{K} \sum_{n=0}^{\frac{m-1-\delta_m}{2}} h_K v_0^{(K-m)} a^m \binom{K}{m} \left\{ \left(\frac{1}{2}\right)^{m-1} \binom{m}{n} \cos(m-2n)\phi \right.$$

$$\left. + \binom{m}{m/2} \frac{\delta_m}{2^m} \right\}, \qquad K \geq m, \qquad m > 2n \qquad (A\,1)$$

where

$$\delta_x = \begin{cases} 0, & x: \text{ odd} \\ 1, & x: \text{ even} \end{cases} \qquad (A\,2)$$

so that

$$i_a(v_0 + a \cos \phi) = \sum_{K=0}^{5} \sum_{m=0}^{K} h_K v_0^{(K-m)} a^m \binom{K}{m} \binom{m}{m/2} \frac{\delta_m}{2^m}$$

$$= \sum_{K=0}^{5} h_K v_0^K + \frac{1}{2} \sum_{K=2}^{5} \binom{K}{2} h_K v_0^{(K-2)} a^2 + \frac{3}{8} \sum_{K=4}^{5} \binom{K}{4} h_K v_0^{(K-4)} a^4 \qquad (A\,3)$$

and

$$\left[i_a(v_0 + a \cos \phi) \right]_{\cos \phi} = \left\{ \sum_{K=1}^{5} K h_K v_0^{(K-1)} a + \frac{3}{4} \sum_{K=3}^{5} \binom{K}{3} h_K v_0^{(K-3)} a^3 \right.$$

$$\left. + \frac{5}{8} h_5 a^5 \right\} \cos \phi = C_1(a\,;\,v_0) \cos \phi . \qquad (A\,4)$$

Appendix II[1]

$$f(a \cos \phi,\ -a \sin \phi) = -Q r i_a(v_0 + a \cos \phi) + \varphi(a \cos \phi) a \sin \phi . \qquad (A\,5)$$

Now put

$$\varPhi(v) = \int_0^v \varphi(v) dv , \qquad (A\,6)$$

then

$$\Phi(v) = \int_0^v \left\{ 1 + QZ \frac{di(v_0 + v)}{d(v_0 + v)} \right\} dv$$
$$= v + QZi(v_0 + v) \,. \tag{A 7}$$

From Eq. (A 7), $\Phi(a \cos \phi)$ can be obtained as

$$\Phi(a \cos \phi) = a \cos \phi + QZ \sum_{K=0}^{5} h_K(v_0 + a \cos \phi)$$

$$= a \cos \phi + QZ \sum_{K=0}^{5} \sum_{m=0}^{K} \sum_{n=0}^{\frac{m-1-\delta_m}{2}} h_K v_0^{(K-m)} \cdots$$

$$\cdot a^m \binom{K}{m} \left\{ \left(\frac{1}{2} \right)^{m-1} \binom{m}{n} \cos(m - 2n)\phi + \binom{m}{m/2} \frac{\delta_m}{2^m} \right\} \,. \tag{A 8}$$

By partial differentiating $\Phi(a \cos \phi)$ with respect to ϕ,

$$\frac{\partial \Phi(a \cos \phi)}{\partial \phi} = -a \sin \phi - QZ \sum_{K=0}^{5} \sum_{m=0}^{K} \sum_{n=0}^{\frac{m-1-\delta_m}{2}} h_K v_0^{(K-m)} \cdot$$

$$\cdot a^m \binom{K}{m} (m - 2n) \left(\frac{1}{2} \right)^{m-1} \binom{m}{n} \sin(m - 2n)\phi$$

$$= \frac{\partial \Phi(a \cos \phi)}{\partial (a \cos \phi)} \cdot \frac{\partial (a \cos \phi)}{\partial \phi} = \varphi(a \cos \phi) \cdot (-a \sin \phi) \,. \tag{A 9}$$

From this equation

$$\varphi(a \cos \phi) a \sin \phi = a \sin \phi + QZ \sum_{K=0}^{5} \sum_{m=0}^{K} \sum_{n=0}^{\frac{m-1-\delta_m}{2}} h_K v_0^{(K-m)} \cdot$$

$$\cdot a^m \binom{K}{m} (m - 2n) \left(\frac{1}{2} \right)^{m-1} \binom{m}{n} \sin(m - 2n)\phi \,. \tag{A 10}$$

The component of $\sin \phi$ of Eq. (A 10) is

$$\left[\varphi(a \sin \phi) a \sin \phi \right]_{\sin \phi} = \left\{ a + QZ C_1(a \,;\, v_0) \right\} \sin \phi$$
$$= S_1(a \,;\, v_0) \sin \phi \,, \tag{A 11}$$

where

$$S_1(a \,;\, v_0) = a + QZ C_1(a \,;\, v_0)$$

By using the above equations, $A_1(a)$ and $B_1(a)$ of Eqs. (15 a, b) can be calculated as

$$A_1(a) = -\frac{1}{2\pi} \int_0^{2\pi} f(a \cos \phi, \, -a \sin \phi) \sin \phi \, d\phi$$

$$= -\frac{1}{2\pi}\int_0^{2\pi}\Big[\varphi(a\sin\phi)a\sin\phi\Big]_{\sin\phi}\cdot\sin\phi\,d\phi$$

$$= -\frac{1}{2}S_1(a\,;\,v_0) \tag{A 12 a}$$

and

$$B_1(a) = -\frac{1}{2\pi}\int_0^{2\pi}f(a\cos\phi,\ -a\sin\phi)\cos\phi\,d\phi$$

$$= \frac{Qr}{2\pi a}\int_0^{2\pi}\Big[i_a(v_0+a\cos\phi)\Big]_{\cos\phi}\cdot\cos\phi\,d\phi$$

$$= \frac{Qr}{2a}C_1(a\,;\,v_0). \tag{A 12 b}$$

Eqs. (A 12 a, b) are the same with Eqs. (16 a, b) respectively.

Appendix III

From Eq. (A 1),

$$i_0(a) = \sum_{K=0}^{5}h_K v_0^{K}+\frac{1}{2}\sum_{K=0}^{5}\binom{K}{2}h_K v_0^{(K-2)}a^2$$

$$+\frac{3}{8}\sum_{K=4}^{5}\binom{K}{4}h_K v_0^{(K-4)}a^4, \tag{A 13 a}$$

$$i_1(a) = a\Big\{\sum_{K=1}^{5}K h_K v_0^{(K-1)}+\frac{3}{4}\sum_{K=3}^{5}\binom{K}{3}h_K v_0^{(K-3)}a^2$$

$$+\frac{5}{8}h_5 a^4\Big\}, \tag{A 13 b}$$

$$i_2(a) = a^2\Big\{\frac{1}{2}\sum_{K=2}^{5}\binom{K}{2}h_K v_0^{(K-2)}+\frac{1}{2}\sum_{K=4}^{5}\binom{K}{4}h_K v_0^{(K-4)}a^2\Big\}, \tag{A 13 c}$$

$$i_3(a) = a^3\Big\{\frac{1}{4}\sum_{K=3}^{5}\binom{K}{3}h_K v_0^{(K-3)}+\frac{5}{16}h_5 a^2\Big\}, \tag{A 13 d}$$

$$i_4(a) = \frac{1}{8}\sum_{K=4}^{5}\binom{K}{4}h_K v_0^{(K-4)}a^4 \tag{A 13 e}$$

and

$$i_5(a) = \frac{1}{16}h_5 a^5. \tag{A 13 f}$$

Appendix IV

$$\frac{\partial i(a\cos\phi)}{\partial a} = i'(a\cos\phi)\cdot\cos\phi = \sum_{n\geqslant 0}\frac{di_n(a)}{da}\cdot\cos n\phi, \qquad \text{(A 14 a)}$$

$$\frac{\partial i(a\cos\phi)}{\partial\phi} = i'(a\cos\phi)\cdot(-a\sin\phi) = -\sum_{n\geqslant 0}ni_n(a)\cdot\sin n\phi.$$

$$\text{(A 14 b)}$$

By using Eq. (A 14 a),

$$I_{cn}(a) = \frac{1}{\pi}\int_0^{2\pi}\varDelta\cdot i'(a\cos\phi)\cdot\cos\phi\,d\phi$$

$$= \sum_{n\mp 1}\frac{i_n(a)}{|y_0(n\omega)|}\cdot\frac{1}{\pi}\int_0^{2\pi}i'(a\cos\phi)\cdot\cos\phi\cdot\cos\{n\phi-\phi(n\omega)\}d\phi$$

$$= \sum_{n\mp 1}\frac{i_n(a)}{|y_0(n\omega)|}\cdot\frac{1}{\pi}\int_0^{2\pi}\sum_{K\geqslant 0}\frac{di_K(a)}{da}\cos K\phi\{\cos n\phi\cos\phi(n\omega)$$

$$-\sin n\phi\sin\phi(n\omega)\}d\phi$$

$$= \sum_{n\mp 1}\frac{i_n(a)}{|y_0(n\omega)|}\cdot\frac{di_n(a)}{da}\cdot\cos\phi(n\omega)$$

$$= \sum_{n\mp 1}\frac{1}{2}\cdot\frac{1}{|y_0(n\omega)|}\cdot\frac{di_n^2(a)}{da}\cdot\cos\phi(n\omega), \qquad \text{(A 15 a)}$$

and by using Eq. (A 14 b),

$$I_{sn}(a) = \frac{1}{\pi}\int_0^{2\pi}\varDelta\cdot i'(a\cos\phi)\sin\phi\,d\phi$$

$$= \frac{1}{\pi}\sum_{n\mp 1}\frac{i_n(a)}{|y_0(n\omega)|}\cdot\int_0^{2\pi}i'(a\cos\phi)\sin\phi\{\cos n\phi\cos\phi(n\omega)$$

$$-\sin n\phi\sin\phi(n\omega)\}d\phi$$

$$= \sum_{n\mp 1}\frac{1}{|y_0(n\omega)|}\cdot\frac{ni_n^2(a)}{a}\cdot\sin\phi(n\omega). \qquad \text{(A 15 b)}$$

References

1) Н. Н. БОТОЛЮБОВ И Ю. А. МИТРОПОЛЬСКИЙ: "Asymptotic methods in analysis of non-linear vibrations".

2) T. Kurobe, Y. Ogawa and S. Kondo: "On the hysteresis phenomena of the Esaki-diode oscillator". The records of the General Meeting of I.E., I.E.C., I.I. and I.T.E. of Japan; No. 1635, April, 1963.